New interpretation of the spreading evolution of the Knipovich Ridge derived from aeromagnetic data

M.-A. Dumais [1,2] L. Gernigon,[1] O. Olesen,[1] S.E. Johansen[2] and M. Brönner[1]

[1]*Geological Survey of Norway,* 7040 *Trondheim, Norway.* E-mail: *marie-andree.dumais@ngu.no*
[2]*Department of Geoscience and Petroleum, Norwegian University of Science and Technology,* 7031 *Trondheim, Norway*

SUMMARY

Insights into the spreading evolution of the Knipovich Ridge and development of the Fram Strait are revealed from a recent aeromagnetic survey. As an ultraslow spreading ridge in an oblique system located between the Svalbard–Barents Sea and the Northeast Greenland rifted margins, the dynamics of the Knipovich Ridge opening has long been debated. Its 90° bend with the Mohns Ridge, rare in plate tectonics, affects the evolution of the Fram Strait and motivates the study of crustal deformation with this distinctive configuration. We identified magnetic isochrons on either side of the present-day Knipovich Ridge. These magnetic observations considerably reduce the mapped extent of the oceanic domain and question the present understanding of the conjugate rifted margins. Our analysis reveals a failed spreading system before a major spreading reorganization of the Fram Strait gateway around magnetic chron C6 (circa 20 Ma).

Key words: Arctic region; Magnetic anomalies: modelling and interpretation; Mid-ocean ridge processes.

INTRODUCTION

The Fram Strait is a key region for the understanding of the rift-to-drift evolution between the Northeast Greenland and Svalbard–Barents Sea rifted margins. Linking the Atlantic and Arctic spreading systems, the Knipovich Ridge (KnR) initiated following the complete cessation of the Mid-Labrador Ridge spreading in the Early Oligocene (33.7 Ma, C13; Engen *et al.* 2008; Oakey & Chalmers 2012; Hosseinpour *et al.* 2013; Suckro *et al.* 2013) and the diachronous initiation of the Reykjanes, Ægir and Mohns ridges in the Early Eocene (54 Ma, C24r; Talwani & Eldholm 1977; Gaina *et al.* 2009; Gernigon *et al.* 2019). For decades, the structure and evolution of the Fram Strait have been debated due to the scarce data availability in this remote area. In this study, the Fram Strait evolution is interpreted from new state-of-the-art aeromagnetic data, acquired by the Geological Survey of Norway. We revise models for the spreading evolution of the KnR, clearly identify a ridge jump explaining the asymmetric magnetic signature of the ridge and question the present understanding of the Boreas Basin.

Classified as an ultraslow oblique spreading system (with spreading rates of less than 20 mm yr^{-1}), KnR comprises the Arctic Mid-Ocean Ridge system delimited by the Mohns Ridge (MR; ∼73°50′N) and the Molloy Transform Zone (MTZ; ∼78°30′N) between the Greenland Sea and the Barents Sea realms (Fig. 1). It is surrounded by the Vestbakken Volcanic Province (VVP) and the Hornsund Fault Complex Zone (HFZ) to the east, and by the Boreas and East Greenland basins to the west. At present day, the KnR trend changes from NNW–SSE in the south to N–S in the north, with a 130 km wide escarpment and thick piles of sedimentary rocks along the Svalbard margin (Engen *et al.* 2008). The Fram Strait development initiated after a Late Cretaceous-Eocene rifting event between the Barents Sea and Northeast Greenland. It forms a complex system of conjugate shear margins characterized by distinct crustal, structural and magmatic properties (Faleide *et al.* 2008). During the Palaeocene–Eocene, the oblique rifted margins underwent a brief period of compression leading to the Eurekan–Spitsbergen fold and thrust belts (Piepjohn *et al.* 2016). Northwards, KnR is linked through the MTZ to the Gakkel Ridge (GaR; Glebovsky *et al.* 2006). The Hovgaard Ridge and the East Greenland Ridge, along the Greenland Fracture Zone (GFZ), may include continental fragments preserved within the oceanic domain (Nemčok *et al.* 2016).

In the Norwegian–Greenland Sea, the breakup occurred around 53.9–57.1 Ma (C24r) and propagated progressively to the south towards the juvenile volcanic margins during the Early Eocene (Gernigon *et al.* 2019). After the extinction of the Mid-Labrador Ridge (Labrador Sea) around 33 Ma (C13), the azimuth of the relative motion between Norway and Greenland underwent a counterclockwise rotation from NNW–SSE to WNW–ESE (31–28 Ma, C12-10; Gaina *et al.* 2009). From this reorganization, the ultraslow spreading Ægir Ridge became extinct around C10, subsequently causing the development of the Kolbeinsey Ridge (KoR) and
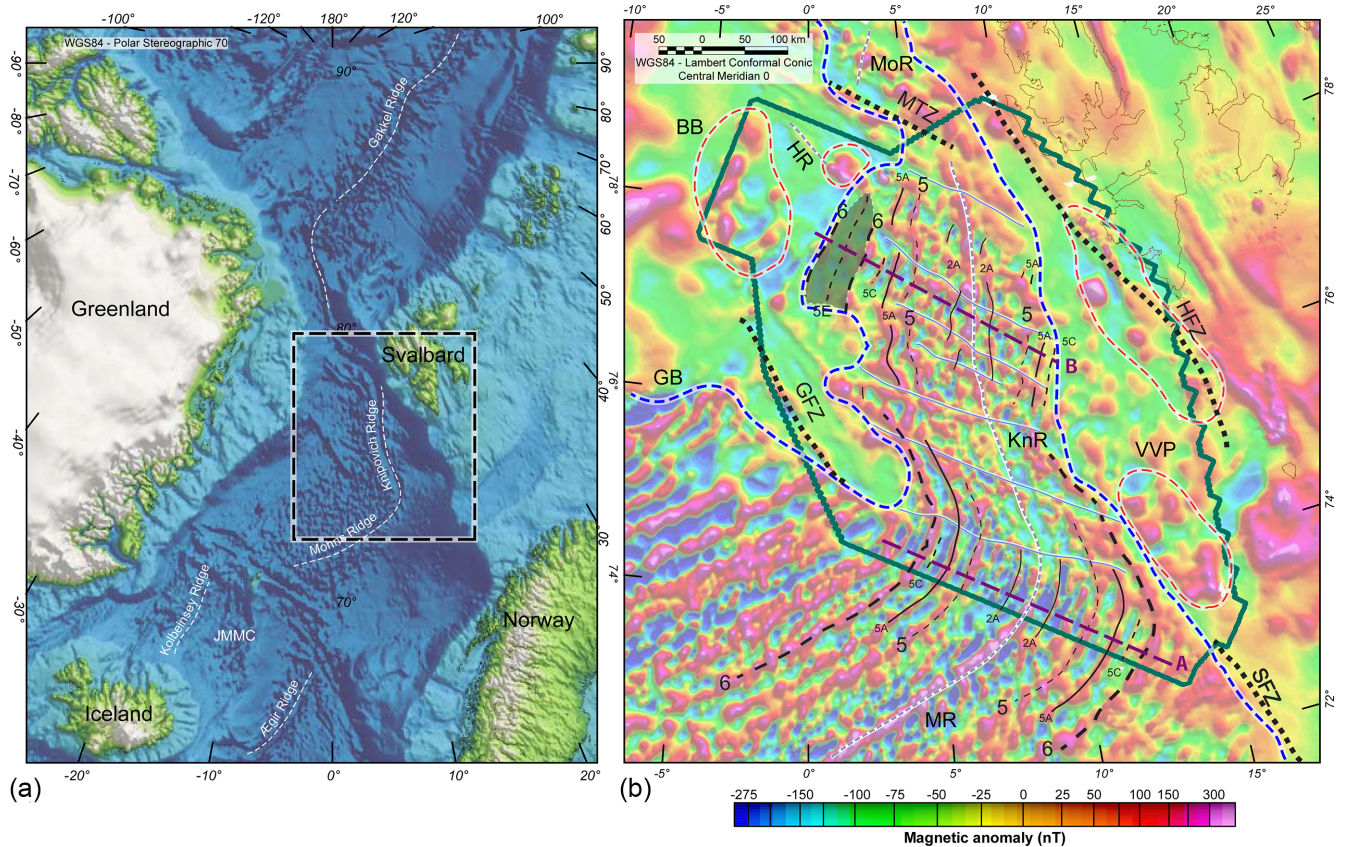
Figure 1. Survey area and aeromagnetic data. (a) Location of the Knipovich Ridge with respect to the North Atlantic realms with SRTM topographic data (Becker *et al.* 2009). (b) The new aeromagnetic data revealed the timing of the breakup (C6) and magmatic events on the eastern side of the ridge. Profiles A and B are in purple. MoR: Molloy Ridge; MTZ: Molloy Transform Zone; HR: Hovgaard Ridge; BB: Boreas Basin; HFZ: Hornsund Fracture Zone; KnR: Knipovich Ridge; GFZ: Greenland Fracture Zone; GB: Greenland Basin; JMMC: Jan Mayen Microplate Complex; VVP: Vestbakken Volcanic Province; MR: Mohns Ridge; SFZ: Senja Fracture Zone. New oceanic fracture zones are displayed with grey lines, new COB demarcation is in dashed blue line and volcanic areas are delimited by the dashed red lines. The abandoned ridge is highlighted in grey shading.

leading to the formation of the Jan Mayen Microplate Complex at ∼24 Ma (C7-6; Blischke *et al.* 2017). To the north, the GaR was initiated at 58–59 Ma (C26n-25r) followed by a spreading rate decrease from C13 (Schreider *et al.* 2019). A 250-km long section of the GaR, north of Svalbard, ending in the Fram Strait, opened much later between C8 and C5 (Glebovsky *et al.* 2006). Similarly, the Molloy Ridge spreading was initiated in the Early Miocene (20 Ma; Srivastava & Tapscott 1986). Earlier studies set the KnR opening at C13 (∼33 Ma; Talwani & Eldholm 1977), between C23 and C13 (Faleide *et al.* 2008) or between C24 and C13 (Nemčok *et al.* 2016). Our new interpretation of the magnetic isochrons significantly changes the time of the KnR spreading initiation and consequently the location of the continent–ocean boundary (COB) compared to previous studies.

DATA

Aeromagnetic survey

The aeromagnetic data were acquired in the summers of 2016 and 2018 during a period of moderate to low diurnal magnetic activity (Novatem 2018; Dumais *et al.* 2020). Located at high latitude, the survey area is particularly sensitive to diurnal noise. Magnetic base station recordings from five locations provided by the Tromsø

Geophysical Observatory and the Technical University of Denmark were used, ensuring high confidence of the data set. Flown at the low altitude of 120 m, with flight lines oriented at 121–301° from N and with a 5500 m line spacing, the data were corrected for the 12th IGRF Field (Thébault *et al.* 2015) and standard levelling using the adjustment of the line intersections (Whitham & Niblett 1961; Reford & Sumner 1964; Nabighian *et al.* 2005) was applied. The lines were designed perpendicular to the ridge axis and the expected spreading anomalies, optimizing the identification of magnetic isochrons. The compilation was completed with existing data from the surrounding areas: GaR, Boreas Basin, Barents Sea and Svalbard (Jokat *et al.* 2008; Olesen *et al.* 2010; Jokat *et al.* 2016).

METHODS

Spreading rate model

ModMag (Mendel *et al.* 2005) was used to map the spreading on profiles A and B (Fig. 2), chosen for their complete signature of the spreading. Profile A was tested for an upper crust of a constant 1 km thickness (Johansen *et al.* 2019), representative of the basalt layer 2A (Fig. 2a), allowing a good agreement between the modelled and observed anomalies. Since the magnetic signature is continuous from MR to KnR at the bend, initial identification of the
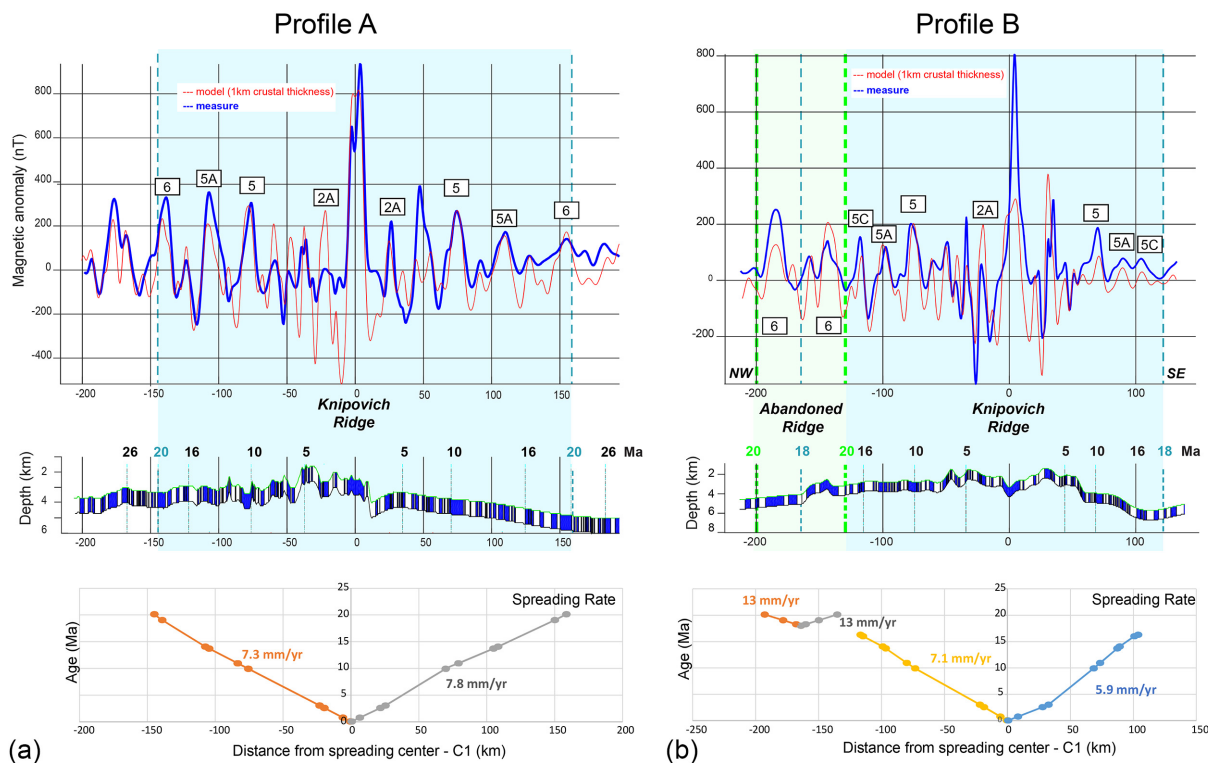
Figure 2. Spreading models (profiles A and B, as identified in Fig. 1) for an upper crust of 1 km. The spreading is faster towards west on profile B while slightly faster towards east on profile A. The presence of an abandoned ridge at C5E-C5C (18 Ma) explains the strong asymmetry of profile B.

magnetic isochrons were derived from the MR interpretation (Vogt *et al.* 1986; Engen *et al.* 2008) to model Profile A consistently. All parameters were adjusted by iteration to fit the observed data. To ensure a data fit with the model and account for the burial of the source layer, a sediment thickness was estimated from Engen *et al.* (2006).

Plate reconstruction

The plate reconstruction was carried out with *GPlates 2.2* (Müller *et al.* 2018), allowing the visualization and the manipulation of the plate-tectonic reconstruction using available refined plate boundaries and isochron layers (Matthews *et al.* 2016; Gernigon *et al.* 2019). The new magnetic isochrons were defined with the magnetic gridded data and their respective age were identified from the spreading rate model results along profiles A and B. Geometries were edited in accordance with the magnetic interpretation.

RESULTS

Oceanic domain of the Fram Strait

The new aeromagnetic data reflect the complexity of the Fram Strait development and the oblique character of the KnR. Spatial analysis of patterns in the frequency content of the data reveals the crustal affinities and demarks various crustal domains (Fig. 1). Areas displaying high-frequency striped magnetic anomalies delineate the oceanic domain, characterized by magnetized basalt and magnetic isochrons correlated to the chronostratigraphic chart of Ogg

(2012). Magnetic isochron C6 is assigned to the first unambiguous striped anomaly. C5A, C5 and C1 are also assigned as they extend continuously from the MR to the KnR. Modelling of the high-frequency magnetic isochrons with 1 km upper crustal thickness replicates the magnetic signature with high confidence and gives new insights in the spreading history. The data set captures previously unresolved magnetic isochrons, for example, C2A, facilitating a more detailed and better constrained plate reconstruction. These also characterize the oceanic domain, where C6 demarks the first unambiguous magnetic isochron and revises the location of the expected COB landwards of C6. Unlike its adjacent ridges, MR and GaR, the KnR magnetic signature suggests the presence of several asymmetrical discontinuous spreading segments (Fig. 1). Not previously observed on bathymetric data, new oceanic transfer faults between these segments are delineated, running parallel to the GFZ and the MTZ but perpendicular to the spreading anomalies.

Rifted margin, transitional domain and continental fragments

Outside the oceanic domain, the magnetic signature mainly contains intermediate-to-long wavelength anomalies without evidence of any magnetic isochrons, which is characteristic of continental or transitional crustal domains. Intermediate-size round anomalies (20–50 km diameter) found in the VVP and along the HFZ most likely express the volcanism of the Svalbard margin. On the Greenland margins, intermediate-frequency magnetic anomalies are observed along the GFZ, MTZ and the Hovgaard Ridge (Fig. 1). The new location of the COB extends the continental domain towards the

Hovgaard and East Greenland Ridges. It also envelopes the Boreas Basin which mainly shows characteristics of a continental domain. These continental fragments appear strongly linked to the continent without indications of strong discontinuities.

Spreading rates and instability: evidence of a failed spreading system

With the magnetic data, the oceanic fracture zones are clearly delineated, highlighting the segmented nature of the spreading system. Furthermore, some of these segments exhibit evidence for strong asymmetrical spreading, while others show small amplitudes and poor magnetization (Fig. 1b), which underlines the complexity and heterogeneity of this ultraslow spreading system in a sheared setting. The bathymetric data indicate that the strike of the KnR varies from 347°, at the junction with MR, to 002°, at the MTZ junction (Curewitz *et al.* 2010). On the magnetic data, the direction of the visible spreading anomalies is 300° (Fig. 1). Given the orientation of plate motion and the large rotation in the ridge-crest strike through the study area, the obliquity varies from ~45°, at MR, to ~30°, at MTZ. The thick sedimentary cover of the Barents Sea fan (Engen *et al.* 2006) on the eastern flank of KnR means that the magnetic sources in the crust are further away from the magnetic measurements. This causes the presence of wider anomalies compared to their conjugate. According to the model, the extent of the spreading anomalies remains slightly asymmetric, implying the spreading evolution with moderately faster rates towards east at the bend connecting MR and KnR (Fig. 2). Between profile A and B, the spreading rates decrease east of KnR, while they appear to keep similar rates on the west side (Fig. 2b). Thus, around N76°, the asymmetry reverses, and the western oceanic domain becomes apparently larger.

Consequently, the segment between N76° and N78° reveals a pronounced asymmetry with a broader extent of the oceanic domain west of the present-day KnR (Fig. 2). The new magnetic data indicate the presence of an atypical and failed spreading system, immediately west of the current ridge and east of the continental Boreas Basin, explaining the evident asymmetry of the spreading. The abandoned ridge model is favoured over a model with one single highly asymmetric system. The latter model would require much faster spreading towards the west, an unequal number of magnetic isochrons on either side of the ridge and very different spreading rates from north to south. While sedimentary cover prevails the direct observation of a ridge-typical bathymetric depression, both, top basement interpretation from seismic data (Hermann & Jokat 2013) and the new magnetic data underline the high potential for the existence of an abandoned rift valley. Thus, the failed spreading system with a ridge jump hypothesis was tested along profile B located in the most asymmetric segment of the KnR. The final model presents slower spreading rates particularly towards the east and confirms the presence of an atypical oceanic domain initiated at C6. In addition, it suggests a ridge jump between C5E and C5C, required to explain this asymmetry (Figs 1 and 2).
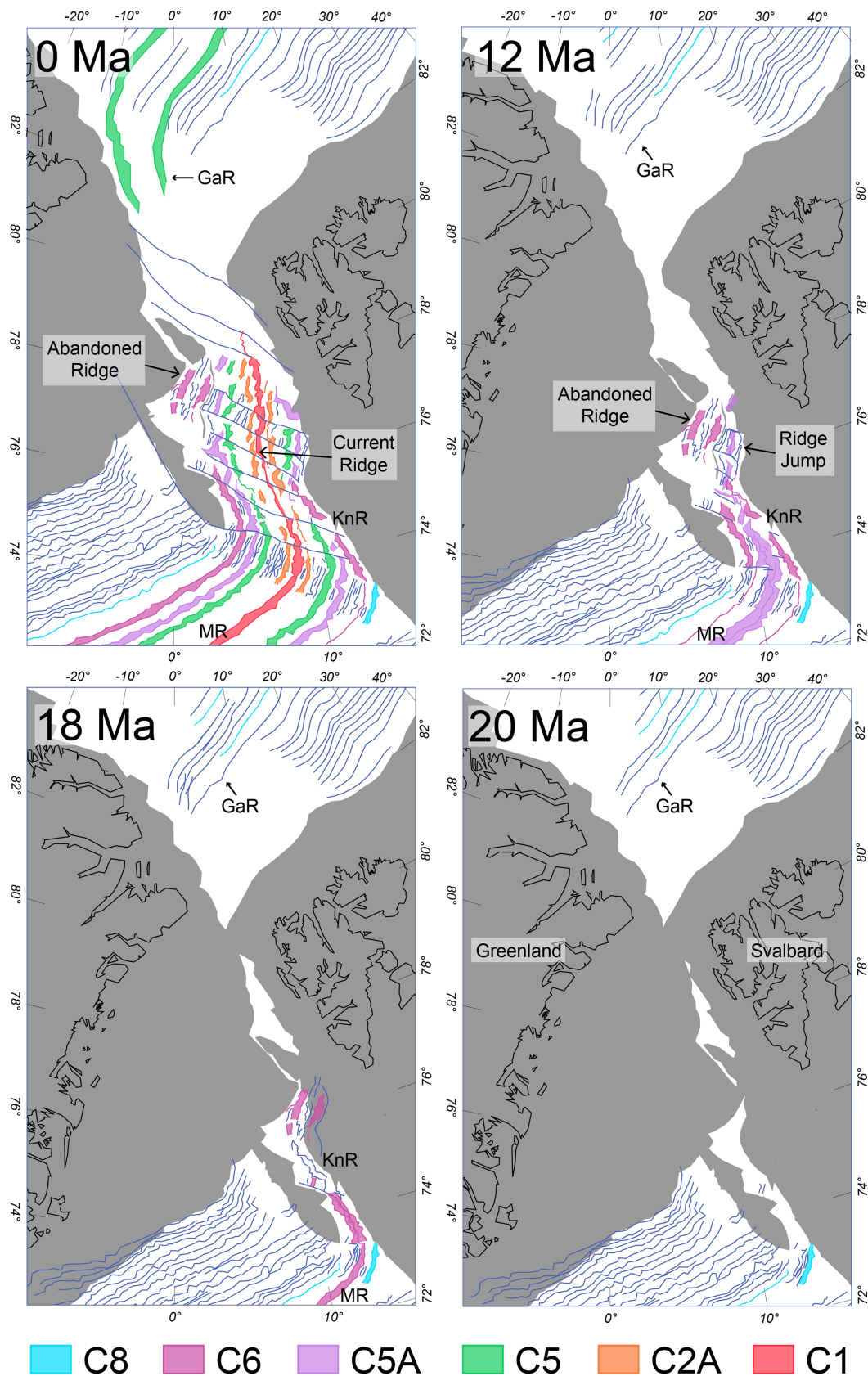
Reconstruction of the Fram Strait

In our reconstruction of the Fram Strait (Figs 1–3), the spreading initiated at C6 (20 Ma). Around 18 Ma (C5E-C5C), the section between N77° and N78° was abandoned and migrated to the east where the spreading continued, forming today's KnR (Fig. 4). Within this new section, the spreading becomes faster towards the Boreas Basin. Between N75° and N76°, the striped anomalies disappear ridgewards of C5 (10 Ma), implying relatively weak magnetization of the crust, which needs further investigation. The segment linking the MTZ shows a magnetic isochron corresponding to C1, with no further striped anomalies parallel to it, suggesting an opening more recent than C2A. Seafloor spreading anomalies allow us to delineate discrete corridors with contrasting histories of spreading rate variation and asymmetry, caused by ridge abandonment and migration episodes. The edges of these corridors appear to be marked by oceanic fracture zones.
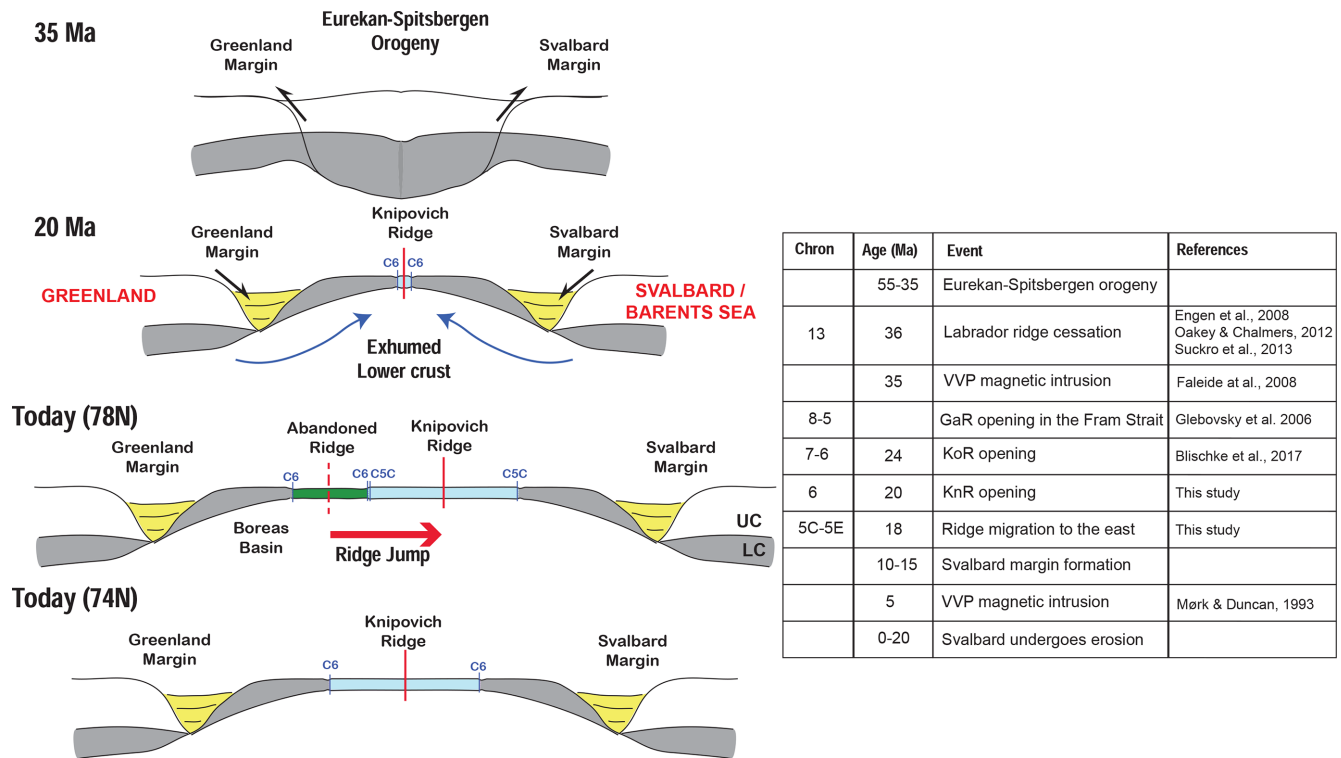
DISCUSSION

Our results demark the much-debated COB in the North Atlantic and Arctic Oceans and in the Fram Strait in particular (Breivik *et al.* 1999; Voss & Jokat 2007; Faleide *et al.* 2008; Gernigon *et al.* 2019), and confirm the opening of the KnR initiated at 20 Ma (C6) where the first unambiguous magnetic anomaly appears. The KnR lies oblique to the MR and developed after the opening of the Norwegian–Greenland Sea and the Eurasian Basin which had already initiated in the Early Eocene (Brozena *et al.* 2003) and after the complete extinction of the Mid-Labrador Ridge at C13 (Gaina *et al.* 2009; Oakey & Chalmers 2012; Hosseinpour *et al.* 2013; Suckro *et al.* 2013). This coincides with the opening of the Molloy Ridge (20 Ma; Trulsvik *et al.* 2011) and KoR (C7-6; Blischke *et al.* 2017), and the GaR penetrating in the Fram Strait (C8-5; Glebovsky *et al.* 2006).

East of KnR, the new COB is closer to the ridge by up to 150 km compared to the previous interpretations (Breivik *et al.* 1999). The oceanic crust, enclosed by magnetic isochrons C6, is relatively thin, up to 5 km (Johansen *et al.* 2019), and characterized by remanently magnetized basalts. The crustal sections between magnetic isochrons C6 and the rifted margins, on either side of the KnR, are representative of a stretched continental crust due to the apparent absence of striped magnetic anomalies associated with an authentic oceanic crust. The presence of rounded, intermediate-size magnetic anomalies suggests the occurrence of intrusive magmatic bodies in this area. Therefore, we postulate the presence of an exhumed and intruded lower continental crust before the development of an oceanic accretion in the Fram Strait (Fig. 4). Along the West Barents Sea margin, magmatic intrusions were likely emplaced in two phases in the VVP, estimated at 35 Ma from seismic observations (Faleide *et al.* 2008) and 5 Ma from borehole age dating (Mørk & Duncan 1993). On either side of the ridge, the basement shares affinities despite magmatism being mostly constrained to the West Barents shear margin. Magmatism may have occurred before and after the KnR initiation (Fig. 1). Recent studies have shown the possibility for intruded lower continental crust to flow laterally before the establishment of steady-state oceanic crust (Foulger *et al.* 2019; Guan *et al.* 2019; Bécel *et al.* 2020; Yuan *et al.* 2020). The intermediate-to-long wavelength magnetic anomalies observed continent-ward of C6 may represent a similar intruded lower crust instead of an oceanic crust. This interpretation challenges previous interpretations of the nature and lateral extent of the conjugate margins. Further investigation is required to fully understand the tectonic processes by acquiring additional seismic data covering the different crustal domains, revisiting the existing seismic interpretation of the area, and developing a thermal model of the mantle.

Figure 3. Reconstruction of the opening of the KnR. The ridge in the Boreas Basin is abandoned at 18 Ma and jumped eastwards towards Svalbard (GaR: Gakkel Ridge; KnR: Knipovich Ridge; MR: Mohns Ridge). Oceanic fracture zones, lineaments and magnetic isochrons are shown in blue. The plate boundary and magnetic isochron layers displayed along the KnR have been extracted from the new data set. The topography, plate boundary and magnetic isochron layers outside the KnR uses previous studies (Amante & Eakins 2009; Matthews *et al.* 2016; Gernigon *et al.* 2019).

Chron	Age (Ma)	Event	References
	55-35	Eurekan-Spitsbergen orogeny	
13	36	Labrador ridge cessation	Engen et al., 2008 Oakey & Chalmers, 2012 Suckro et al., 2013
	35	VVP magnetic intrusion	Faleide at al., 2008
8-5		GaR opening in the Fram Strait	Glebovsky et al. 2006
7-6	24	KoR opening	Blischke et al., 2017
6	20	KnR opening	This study
5C-5E	18	Ridge migration to the east	This study
	10-15	Svalbard margin formation	
	5	VVP magnetic intrusion	Mørk & Duncan, 1993
	0-20	Svalbard undergoes erosion	

Figure 4. Schematic of the opening of the KnR. At 78°N, the ridge in the Boreas Basin is abandoned and jumped eastwards to become present-day Knipovich Ridge. At 74°N, the ridge has continuously opened since breakup around 20 Ma. UC: Upper crust; LC: Lower crust.

CONCLUSION

Our aeromagnetic data shed light on the development and crustal deformation to the rare configuration of two ultraslow spreading segments of the NE Atlantic spreading system intersecting at a 90° angle:

(1) Despite this 90° bend between the MR and the KnR, the opening at the southern section of the KnR is continuous from the Monhs Ridge, underlining the eminent transtensional plate motion in the high Arctic.

(2) Our study sets the KnR opening at 20 Ma and suggests the presence of numerous oceanic fracture zones and a broad continent–ocean transition interpreted as exhumed lower continental material.

(3) The presence of a failed oceanic basin east of the Boreas Basin with a thin crust explains the peculiar strong asymmetry of the spreading system. Consequently, a ridge jump is inferred in the Fram Strait around 18 Ma.

(4) The KnR opening occurred shortly after of the Kolbeinsey Ridge opening and Gakkel Ridge prolongation. It may indicate a common link of mid-Atlantic ridge segments allowing a synchronous initiation of breakup at several locations of the North Atlantic–Arctic realm.

REFERENCES

Amante, C. & Eakins, B.W., 2009. ETOPO1 arc-minute global relief model: procedures, data sources and analysis. NOAA Technical Memorandum NESDIS NGDC-24, *National Geophysical Data Center, NOAA,* **10,** V5C8276M.

Bécel, A., Davis, J.K., Shuck, B.D., Van Avendonk, H.J.A. & Gibson, J.C., 2020. Evidence for a prolonged continental breakup resulting from slow extension rates at the Eastern North American Volcanic Rifted Margin, *J. geophys. Res.,* **125,** e2020JB020093, doi:10.1029/2020jb020093.

Becker, J.J. *et al.*, 2009. Global bathymetry and elevation data at 30 Arc seconds resolution: SRTM30_PLUS, *Mar. Geod.,* **32,** 355–371.

Blischke, A., Gaina, C., Hopper, J.R., Péron-Pinvidic, G., Brandsdóttir, B., Guarnieri, P., Erlendsson, Ö. & Gunnarsson, K., 2017. The Jan Mayen microcontinent: an update of its architecture, structural development and role during the transition from the Ægir Ridge to the mid-oceanic Kolbeinsey Ridge, *Geol. Soc., London, Spec. Publ.,* **447,** 299–337.

Breivik, A.J., Verhoef, J. & Faleide, J.I., 1999. Effect of thermal contrasts on gravity modeling at passive margins: results from the western Barents Sea, *J. geophys. Res.,* **104,** 15 293–15 311.

Brozena, J.M., Childers, V.A., Lawver, L.A., Gahagan, L.M., Forsberg, R., Faleide, J.I. & Eldholm, O., 2003. New aerogeophysical study of the Eurasia Basin and Lomonosov Ridge: implications for basin development, *Geology,* **31,** 825.

Curewitz, D., Okino, K., Asada, M., Baranov, B., Gusev, E. & Tamaki, K., 2010. Structural analysis of fault populations along the oblique, ultra-slow spreading Knipovich Ridge, North Atlantic Ocean, 74°30′N-77°50′N, *J. Struct. Geol.,* **32,** 727–740.

Dumais, M.A., Olesen, O., Gernigon, L., Brönner, M., Lim, A. & Johansen, S.E., 2020. Knipovich Ridge Aeromagnetic Survey 2016: processing and interpretation, NGU-rapport 2020.030.

Engen, Ø., Faleide, J.I. & Dyreng, T.K., 2008. Opening of the Fram Strait gateway: a review of plate tectonic constraints, *Tectonophysics,* **450,** 51–69.

Engen, Ø., Frazer, L.N., Wessel, P. & Faleide, J.I., 2006. Prediction of sediment thickness in the Norwegian-Greenland Sea from gravity inversion, *J. geophys. Res.,* **111,** B11403, doi:10.1029/2005JB003924.

Faleide, J.I., Tsikalas, F., Breivik, A., Mjelde, R., Ritzmann, O., Engen, Ø., Wilson, J. & Eldholm, O., 2008. Structure and evolution of the continental margin off Norway and Barents Sea, *Episodes,* **31,** 82–91.

Foulger, G.R. *et al.*, 2019. The Iceland Microcontinent and a continental Greenland-Iceland-Faroe Ridge, *Earth Sci. Rev.,* 102926, doi:10.1016/j.earscirev.2019.102926.

Gaina, C., Gernigon, L. & Ball, P., 2009. Palaeocene—recent plate boundaries in the NE Atlantic and the formation of the Jan Mayen microcontinent, *J. Geol. Soc.,* **166,** 601–616.

Gernigon, L., Franke, D., Geoffroy, L., Schiffer, C., Foulger, G.R. & Stoker, M., 2019. Crustal fragmentation, magmatism, and the diachronous opening of the Norwegian-Greenland Sea, *Earth Sci. Rev.,* doi:10.1016/j.earscirev.2019.04.011.

Glebovsky, V.Y., Kaminsky, V.D., Minakov, A.N., Merkur'ev, S.A., Childers, V.A. & Brozena, J.M., 2006. Formation of the Eurasia Basin in the Arctic Ocean as inferred from geohistorical analysis of the anomalous magnetic field, *Geotectonics,* **40,** 263–281.

Guan, H., Geoffroy, L., Gernigon, L., Chauvet, F., Grigné, C. & Werner, P., 2019. Magmatic ocean–continent transitions, *Mar. Pet. Geol.,* **104,** 438–450.

Hermann, T. & Jokat, W., 2013. Crustal structures of the Boreas Basin and the Knipovich Ridge, North Atlantic, *Geophys. J. Int.,* **193,** 1399–1414.

Hosseinpour, M., R.D., M., Williams, S.E. & Whittaker, J.M., 2013. Full-fit reconstruction of the Labrador Sea and Baffin Bay, *Solid Earth,* **4,** 461–479.

Johansen, S.E., Panzner, M., Mittet, R., Amundsen, H.E.F., Lim, A., Vik, E., Landrø, M. & Arntsen, B., 2019. Deep electrical imaging of the ultraslow-spreading Mohns Ridge, *Nature,* **567,** 379–383.

Jokat, W., Geissler, W. & Voss, M., 2008. Basement structure of the north-western Yermak Plateau, *Geophys. Res. Lett.,* **35,** doi:10.1029/2007gl032892.

Jokat, W., Lehmann, P., Damaske, D. & Bradley Nelson, J., 2016. Magnetic signature of North-East Greenland, the Morris Jesup Rise, the Yermak Plateau, the central Fram Strait: constraints for the rift/drift history between Greenland and Svalbard since the Eocene, *Tectonophysics,* **691,** 98–109.

Matthews, K.J., Maloney, K.T., Zahirovic, S., Williams, S.E., Seton, M. & Müller, R.D., 2016. Global plate boundary evolution and kinematics since the late Paleozoic, *Glob. Planet. Change,* **146,** 226–250.

Mendel, V., Munschy, M. & Sauter, D., 2005. MODMAG, a MATLAB program to model marine magnetic anomalies, *Comput. Geosci.,* **31,** 589–597.

Mørk, M.B.E. & Duncan, R.A., 1993. Late Pliocene basaltic volcanism on the Western Barents Shelf margin: implications from petrology and ^{40}Ar-^{39}Ar dating of volcaniclastic debris from a shallow drill core, *Nor. Geol. Tidsskr.,* **73,** I993.

Müller, R.D. *et al.*, 2018. GPlates: building a virtual earth through deep time, *Geochem. Geophys. Geosyst.,* **19,** 2243–2261.

Nabighian, M.N., Grauch, V.J.S., Hansen, R.O., LaFehr, T.R., Li, Y., Peirce, J.W., Phillips, J.D. & Ruder, M.E., 2005. The historical development of the magnetic method in exploration, *Geophysics,* **70,** 33ND–61ND.

Nemčok, M., Sinha, S.T., Doré, A.G., Lundin, E.R., Mascle, J. & Rybár, S., 2016. Mechanisms of microcontinent release associated with wrenching-involved continental break-up; a review, *Geol. Soc., London, Spec. Publ.,* **431,** 323, doi:10.1144/sp431.14.

Novatem, 2018, Knipovich Ridge airborne survey 2016 (KRAS-16)—Technical Report, 32pp.

Oakey, G.N. & Chalmers, J.A., 2012. A new model for the Paleogene motion of Greenland relative to North America: plate reconstructions of the Davis Strait and Nares Strait regions between Canada and Greenland, *J. geophys. Res.,* **117,** doi:10.1029/2011jb008942.

Ogg, J.G., 2012. Geomagnetic polarity time scale, in *The Geologic Time Scale,* pp. 85–113, eds Gradstein, F.M., Ogg, J.G., Schmitz, M.D. & Ogg, G.M., Elsevier, doi:10.1016/b978-0-444-59425-9.00005-6.

Olesen, O. *et al.*, 2010. New aeromagnetic and gravity compilations from Norway and adjacent areas: methods and applications, *Geol. Soc., London, Pet. Geol. Conf. Ser.,* **7,** 559–586.

Piepjohn, K., von Gosen, W. & Tessensohn, F., 2016. The Eurekan deformation in the Arctic: an outline, *J. Geol. Soc.,* **173,** 1007–1024.

Reford, M.S. & Sumner, J.S., 1964. Aeromagnetics, *Geophysics,* **29,** 482–516.

Schreider, A.A., Schreider, A., Sazhneva, A., Kluev, M. & Brehovskih, A., 2019. Kinematic model of development of eastern areas of the Gakkel Mid-Ocean Ridge in the Eurasian Basin of the Arctic Ocean, *Oceanology,* **59,** 133–142.

Srivastava, S.P. & Tapscott, C.R., 1986. Plate kinematics of the North Atlantic, in *The Western North Atlantic Region,* eds Vogt, P.R. & Tucholke, B.E., Geological Society of America.

Suckro, S.K., Gohl, K., Funck, T., Heyde, I., Schreckenberger, B., Gerlings, J. & Damm, V., 2013. The Davis Strait crust—a transform margin between two oceanic basins, *Geophys. J. Int.,* **193,** 78–97.

Talwani, M. & Eldholm, O., 1977. Evolution of the Norwegian–Greenland Sea, *Bull. geol. Soc. Am.,* **88,** 969–999.

Thébault, E. *et al.*, 2015. International geomagnetic reference field: the 12th generation, *Earth Planets Space,* **67,** doi:10.1186/s40623-015-0228-9.

Trulsvik, M., Myklebust, R., Polteau, S. & Planke, S., 2011. *Geophysical Atlas of the East Greenland Basin: Integrated Seismic, Gravity and Magnetic Interpretation,* Volcanic Basin Petroleum Research AS, TGS-NOPEC Geophysical Company.

Vogt, P.R., Fruik, C., Jewett, I., Klitgord, K., Vink, G. & Duncan, R., 1986. *Magnetic anomalies of the North Atlantic Ocean,* Geological Society of America.

Voss, M. & Jokat, W., 2007. Continent–ocean transition and voluminous magmatic underplating derived from *P*-wave velocity modelling of the East Greenland continental margin, *Geophys. J. Int.,* **170,** 580–604.

Whitham, K. & Niblett, E.R., 1961. The diurnal problem in aeromagnetic surveying in Canada, *Geophysics,* **26,** 211–228.

Yuan, X., Korenaga, J., Holbrook, W.S. & Kelemen, P.B., 2020. Crustal structure of the Greenland–Iceland ridge from joint refraction and reflection seismic tomography, *J. geophys. Res.,* **125,** e2020JB019847, doi:10.1029/2020jb019847.